

ISTANBUL TECHNICAL UNIVERSITY ★ GRADUATE SCHOOL OF SCIENCE
ENGINEERING AND TECHNOLOGY

REAL TIME PHOTOGRAMMETRIC MONITORING OF BRIDGES

Ph.D. THESIS

Emin Özgür AVŞAR

Geomatics Engineering Department

Geomatics Engineering Programme

Thesis Advisor: Prof. Dr. Orhan ALTAN

JULY 2014

ISTANBUL TECHNICAL UNIVERSITY ★ GRADUATE SCHOOL OF SCIENCE
ENGINEERING AND TECHNOLOGY

REAL TIME PHOTOGRAMMETRIC MONITORING OF BRIDGES

Ph.D. THESIS

Emin Özgür AVŞAR
(501062602)

Geomatics Engineering Department

Geomatics Engineering Programme

Thesis Advisor: Prof. Dr. Orhan ALTAN

JULY 2014

İSTANBUL TEKNİK ÜNİVERSİTESİ ★ FEN BİLİMLERİ ENSTİTÜSÜ

KÖPRÜLERİN GERÇEK ZAMANLI FOTOGRAMETRİK İZLENMESİ

DOKTORA TEZİ

**Emin Özgür AVŞAR
(501062602)**

Geomatik Mühendisliği Anabilim Dalı

Geomatik Mühendisliği Programı

Tez Danışmanı: Prof. Dr. Orhan ALTAN

TEMMUZ 2014

Emin Özgür AVŞAR, a **Ph.D.** student of ITU **Institute of Science and Technology** student ID **501062602**, successfully defended the **thesis** entitled “**REAL TIME PHOTOGRAMMETRIC MONITORING OF BRIDGES**”, which he prepared after fulfilling the requirements specified in the associated legislations, before the jury whose signatures are below.

Thesis Advisor : **Prof. Dr. Orhan ALTAN**

İstanbul Technical University

Jury Members : **Prof. Dr. Mehmet Ali TAŞDEMİR**

İstanbul Technical University

Prof. Dr. Sıtkı KÜLÜR

İstanbul Technical University

Prof. Dr. Ferruh YILDIZ

Selcuk University

Assoc. Prof. Dr. Devrim AKÇA

Işık University

Date of Submission : 23 May 2014

Date of Defense : 01 July 2014

To my family,

FOREWORD

First of all, it must be clearly stated that it is impossible to make reference to everybody whom I got support during this research.

Early, I would like to thank my supervisor Prof. Dr. Orhan Altan. His valuable insights and directions gave me needful guidance to complete the research and write this thesis. On the other hand, he encouraged me to pursue my own research areas allowing me to expand my horizon.

I also wish to thank Assoc. Prof. Dr. Devrim Akça with whom I collaborated on several occasions during my research. He was key in exposing and pushing me to the topics covered in this thesis. Also I would like to thank Prof. Dr. Mehmet Ali Taşdemir for his valuable guidance and information. To both researchers I am grateful for giving advice on this and more general researches.

Other important persons considering my life in ITU Department of Geomatics are Prof. Dr. Gönül Toz, Prof. Dr. Sıtkı Külür, Prof. Dr. Dursun Zafer Şeker and Assist. Prof. Dr. Zaide Duran whom I like to give my thanks for giving me an opportunity to share their knowledge and the best available information.

I should mention my precious friends; Melis Mine Şener, Esra Erten and Umut Aydar whose presence and friendship enhance the meaning of my life. Without their support and patience, this thesis would not have been completed.

Last, but certainly not least; my deepest gratitude goes to my parents and my sister for their constant encouragement, guidance and total support in my life.

May 2014

Emin Özgür Avşar
(Geomatic Engineer, M. Sc.)

TABLE OF CONTENTS

	<u>Page</u>
FOREWORD	ix
TABLE OF CONTENTS	xi
ABBREVIATIONS	xiii
LIST OF TABLES	xv
LIST OF FIGURES	xvii
SUMMARY	xix
ÖZET	xxi
1. INTRODUCTION	1
1.1 Aim of the Study.....	1
1.2 Structure of the Thesis.....	2
2. STATE OF ART	3
2.1 Deformation Monitoring of Engineering Structures.....	3
2.2 Deformation Analysis Applications of Close Range Photogrammetry.....	4
3. SYSTEM DESIGN	9
3.1 Description of the Used System.....	9
3.1.1 Network design and simulation.....	10
3.1.2 Video camera and camera calibration.....	14
3.1.3 Video-tacheometers.....	18
3.2 Image Acquisition and Synchronization.....	19
3.3 Automatic Target Recognition.....	22
3.3.1 Image segmentation.....	22
3.3.2 Cross correlation.....	23
3.3.3 Sub-pixel positioning.....	23
3.4 Synchronous Matching of Image Pairs.....	24
3.5 Computation of the Object Coordinates of the Targets.....	24
3.6 Spatial Displacement Analysis.....	24
4. APPLICATION	27
4.1 Preliminary Laboratory Experiments and Applications.....	27
4.1.1 Laboratory condition oscillation test.....	27
4.1.2 Test on pull-out deformations of bonded metal anchors embedded in concrete.....	28
4.2 Network Design and Simulation for the Bridge.....	34
4.3 Displacement Analysis of Suspension Bridges by Photogrammetry.....	37
5. CONCLUSIONS	39
REFERENCES	41
CURRICULUM VITAE	45

ABBREVIATIONS

CAD	: Computer Aided Design
CCD	: Charge Coupled Device
CMOS	: Complementary Metal Oxide Semiconductor
EN	: European Norms
EOTA	: European Organisation for Technical Assessment
ETAG	: European Technical Approval Guidelines
FOV	: Field of View
GDH	: General Directorate of Highways
IATS	: Image Assisted Total Station
IEEE	: Institute of Electrical and Electronical Engineers
kN	: KiloNewton
NCC	: Normalised Cross Corelation
USB	: Universal Serial Bus

LIST OF TABLES

	<u>Page</u>
Table 3.1 : Example result of the algorithm.....	12
Table 3.2 : Standard deviations according to number of cameras.	13
Table 3.3 : Standard deviations according to focal length.	14
Table 3.4 : Camera specifications.	15
Table 3.5 : Lens specifications.....	15
Table 3.6 : Calibration results.	17
Table 3.7 : Comparison of the current commercial available IATS.	19
Table 4.1 : Observed displacements for the 16 mm diameter reinforcements.....	32
Table 4.2 : Observed displacements for the 20 mm diameter reinforcements.....	32
Table 4.3 : N_{u_adh} values and displacements.....	34

LIST OF FIGURES

	<u>Page</u>
Figure 3.1 : Flowchart diagram.....	9
Figure 3.2 : Field of view pyramid.	11
Figure 3.3 : Corner points of the field of view pyramid.	11
Figure 3.4 : Diagram for 3 cameras.	13
Figure 3.5 : Basler 402k.	14
Figure 3.6 : Calibration test field.	17
Figure 3.7 : Current commercial available IATS.....	18
Figure 3.8 : Image acquisition code.	20
Figure 3.9 : Part of the written code.....	21
Figure 4.1 : The pendulum setup.	28
Figure 4.2 : Mode of failures of Anchorages (ACI 355, 1991).....	28
Figure 4.3 : Test Field	31
Figure 4.4 : Displacement-Load Curves	33
Figure 4.5 : Examples of load - displacements curves (EOTA, 2008)	33
Figure 4.6 : Initial map of the area	35
Figure 4.7 : Pillars	36
Figure 4.8 : Targets	36
Figure 4.9 : The horizontal displacement of Target 2 and 4	37
Figure 4.10 : The total displacement of Target 2 and 4	37

REAL TIME PHOTOGRAMMETRIC MONITORING OF BRIDGES

SUMMARY

One of the most important objectives of geodetic and photogrammetric measurements is analysing of deformation occurring depending on time, affected factors and strengths on natural and artificial objects. As the result of the carried-out studies and their outcomes, regular inspection and monitoring was proved to provide significant gains on detecting fatigue and deformations that may occur in structural elements. The importance of the early monitoring and identifying studies once again arise with the consideration of repair, maintenance and even the reconstruction costs. Both being the main links of the transportation network and their economic importance; bridge deformations should be monitored continuously.

Like all engineering structures, the aging process affects bridges. In addition, they are exposed to intensive and/or variable loads, variable weather conditions and material fatigue depending on land or rail line that they are in conjunction with. The factors mentioned above are the main components that affect the bridge deformations.

This thesis presents the results of real-time photogrammetric monitoring the structural deformations of the bridges.

For this purpose, a schedule that contains determining convenient camera-lens set, monitoring and target locations, camera calibration, indoor tests of the designed system, onsite measurements of the bridge and photogrammetric evaluation steps was followed. A self-developed Matlab code was used for synchronous image acquisition and photogrammetric evaluation.

For the first indoor test a pendulum established at the laboratory of Geomatics Engineering Department of ITU in order to observe its oscillation. An area of interest of 1200*880 pixels cover the oscillation area of the pendulum was monitored with 24 frames per second. 1200 frames were gathered and object coordinates calculated according to coordinate system of the ITU calibration field to analysis the oscillation of the pendulum.

For the second indoor test it is aimed to determine the displacements of steel reinforcements, embedded into concrete by using chemical anchorages, while applying axial pulling loads by means of monitoring and photogrammetric evaluation. The test field was established in the Construction Materials Laboratory of Istanbul Technical University. Two steel reinforcements with 16 mm diameter and two with 20 mm diameter were observed during the experiment. All of the reinforcements were all embedded in the concrete with a depth of ten times of their diameters within a C30 grade concrete. The process of measurement can be defined as following: measurement of randomly distributed ground controls points, image acquisition under empty load and every 10 bars pressure increasement and offline photogrammetric evaluation. Post-processing evaluation of image pairs for

reinforcements carried-out by using photogrammetric evaluation software. The acquired displacements were measured for every 10 bars pressure increasement.

For the outdoor test the Second Bophorus Bridge was monitored. There cameras were positioned on pillars which are 20 m beside the abutment of the European side. Power supplies were used to supply electricity of the computers and cameras. The field of view of the cameras were examined and due to the storage capacity and time; 2352 pixels horizontally and 800 pixels vertically were determined as the field of view with 12 frame per seconds that indicates 2 seconds for image capturing and approximately 5.5 seconds for data storing. 4800 dataset for the first day and 31968 dataset for the second day were acquired. Cross correlation image matching and segmentation was used to determine targets on the image in sub-pixel accuracy. Object coordinates of the targets were calculated according to photogrammetric evaluation procedure. Research were concluded by calculation and visualization of displacements.

KÖPRÜLERİN GERÇEK ZAMANLI FOTOGRAMETRİK İZLENMESİ

ÖZET

Jeodezik ve Fotogrametrik ölçmelerin en önemli uğraşlarından biri de, zaman ve etki eden kuvvet ve faktörlere bağlı olarak doğal ve yapay objelerde meydana gelen deformasyonların ölçülmesi ve analizidir.

Mühendislik yapılarındaki deformasyonların izlenmesinde takip edilecek temel işlem adımları:

- Deformasyonu izlenecek yapının performansının (durumunun) belirlenmesi,
- Konum doğruluğu gereksinimi ve buna uygun yöntemin seçimi,
- Ölçmelerin türü ve sayısı,
- Ölçmelerde kullanılacak alet ve donanımların seçimi,
- Ölçmelerin yapılması ve verilerin toplanması,
- Verilerin değerlendirilmesi ve analizi,
- Deformasyonların zaman, konum ve frekans bakımından davranışının ortaya konması,
- Modellenmesi,
- Rapor edilmesi

şeklinde sıralanabilir.

Tüm mühendislik yapıları gibi köprüler de yaşlanma sürecinden etkilenmektedir. Buna ek olarak; buldukları kara ya da demir yolu hattına bağlı olarak; yoğun ve/veya değişken yüklere, değişken hava koşullarına ve malzeme yorgunluğuna uğramaktadırlar. Yukarıda sayılan faktörler köprü deformasyonları üzerinde etkili olan temel faktörlerdir.

Düzenli kontrol ve gözlemlenmenin, yapı elemanlarında meydana gelebilecek malzeme yorgunluğu ve deformasyonları tespit etmede önemli kazançlar sağladığı yapılan çalışmalar ve ortaya çıkan sonuçlar neticesinde kanıtlanmış bir gerçektir. Öncül belirleme çalışmalarının yapılmadığı durumlarda ortaya çıkacak bakım-onarım hatta yeniden yapım çalışmalarının maliyetleri de göz önüne alındığında erken izleme ve belirleme çalışmalarının önemi bir kez daha ortaya çıkmaktadır. Gerek ulaşım ağlarının temel bağlantılarından biri olmaları gerekse ekonomik önemleri göz önüne alındığında köprüler üzerinde meydana gelecek deformasyonların sürekli izlenmesi gereklidir.

Asma köprülerde; köprü yapı elemanları olan; ana taşıyıcı kablolarda, taşıyıcı yol yüzeyinde ve pylonlarda hareket/değişim meydana gelir. Bu hareket/değişimleri belirlemek amacıyla; Geleneksel Jeodezik Yöntemler, Takeometre ölçmeleri, Otomatik nivelman, Hidrostatik nivelman, sapma ölçmeleri, elektronik uzunluk ölçer (EDM), Lazer ölçmeleri, Fotogrametrik yöntemler ve Uydu bazlı yöntemler kullanılmaktadır. Bu yöntemlerden elde edilen veriler yardımıyla belirlenen

hareket/değişimlerle; köprü parçalarında oluşan statik ve dinamik stresler ve buna bağlı olarak da köprü elemanlarının yapısal davranışları belirlenir. Erken izleme ve tanımlama çalışmalarının önemi, bakım onarım ve hatta yeniden inşa etme maliyetleri ile bir kez daha karşımıza çıkmaktadır. Bu bağlamda köprü deformasyonları; ulaşım ağlarının ana bağlantıları ve ekonomik öneminden dolayı sürekli izlenmelidir.

Fotogrametrik olarak yapılan köprü deformasyon ölçmeleri 1970'lerin sonlarına doğru başlamıştır. İlk çalışmalarda metrik kameralar (fotogrametrik çalışmalar için özel olarak üretilmiş), yayılmış hedefler (yansıtıcı olmayan), stereoskopik fotogrametrik ağ planı ve analog-analitik değerlendirme işlemleri giderek metrik olmayan kameraların, yansıtıcı hedeflerin, konvergent ağ planların ve dijital fotogrametrik değerlendirme yöntemlerinin kullanımına dönüşmüştür.

Bu tez çalışması köprülerin yapısal deformasyonunda gerçek zamanlı fotogrametrik izlemelerin sonuçlarını sunmaktadır. Yapılacak olan çalışmada; köprü alt yüzeyinde ışık yayan diyotlar (LED-Light Emitting Diode) ile oluşturulacak hedef ağı hem Digital Kamera verileri ile analiz edilmiştir.

Bu amaçla uygun belirlenen bir akış çerçevesinde; uygun kamera lens setinin belirlenmesi, izleme ve hedef noktalarının konumlarının belirlenmesi, kamera kalibrasyonları, tasarlanmış sistemin kapalı alan testleri, test alanı olarak köprüün ölçmeleri ve fotogrametrik değerlendirme adımları izlenmiştir. Çalışma süresince, eş zamanlı görüntü elde etme ve fotogrametrik değerlendirme aşamalarında kullanılmak üzere yapılan bütün programlamalar Matlab programlama dilinde geliştirilmiştir.

İlk kapalı alan testi için İTÜ Geomatik Mühendisliği Bölümü Laboratuvarında salınımını gözlemek üzere bir sarkaç ile çalışılmıştır. Bu amaçla iki adet kamera ile 1200 * 880 piksellik bir gözleme alanı kullanılarak sarkacın salınımını saniyede 24 kare ile izlenmiştir. Elde edilen 1200 görüntü seti, sarkacın salınımını analiz etmek için kullanılmıştır. Çalışma alanının obje koordinatları İTÜ kalibrasyon alanının koordinat sistemine göre hesaplanmıştır.

İkinci kapalı alan testi olarak, izleme ve fotogrametrik değerlendirme ile, kimyasal ankrajlarla betona gömülmüş demir donatıların eksen boyunuca uygulanan çekme yükü altında yer değiştirmelerinin belirlenmesi hedeflenmiştir. Çalışmada kullanılacak test alanı İstanbul Teknik Üniversitesi Yapı Malzemeleri Laboratuvarında kurularak, deney sırasında çaplarının 10'ar katı derinlikte C30 betona gömülü, 16 mm ve 20 mm çapında ikişer demir donatı incelendi. Ölçme süreci; rastgele dağıtılan yer kontrol noktalarının ölçülmesi, sıfır yük altında ve her 10 barlık basınç artışında görüntü elde etme ve çevrim dışı fotogrametrik değerlendirme olarak tanımlanabilir. Donatıların elde edilen görüntü çiftlerinin değerlendirmesi fotogrametrik değerlendirme yazılımları kullanılarak yapılmıştır. Her 10 bar basınç artışı için elde edilen yer değişiklikleri hesaplanmıştır.

Çalışmanın temel amacını oluşturan köprü hareketlerinin gözlemlenmesi için İkinci Boğaz Köprüsü (Fatih Sultan Mehmet Köprüsü) çalışma alanı olarak kullanılmıştır. Bu amaçla, kameralar köprüün Avrupa yakasındaki ayağının bulunduğu bölgede tesis edilen pilyelere konumlandırılmıştır. Kullanılacak hedef noktalarının enerji ihtiyacı için 12 volt akü, akünün şarjı için kablo, aküden hedefe enerji akışını sağlayacak kablodan oluşan bir sistem tasarlanmıştır. Sistem; taşınabilirlik ve köprü alt yüzeyine monte edilebilmesi için plastik bir kutu içerisinde sabitlenmiştir. Toplam 14 adet hedef noktası köprü alt yüzeyine, köprüün bakımı için kullanılan taşıyıcı platform kullanılarak kimyasal malzeme ile yapıştırılmıştır. Bilgisayar ve

kameraların elektrik desteđi için gc kaynakları kullanılmıřtır. Kameraların grř alanı incelenmiř ve depolama kapasitesi ve zamanı gz nne alınarak yatayda 2352 piksel ve dřeyde 800 piksellik bir grnt alanı ve saniyede 12 grnt alımı yapılarak, 2 saniye grnt alımı ve yaklařık 5.5 saniye veri depolama zamanı sađlanmıřtır. Yapılan arazi alıřmasının ilk gn iin 4800 ve ikinci gn iin 31968 veri seti elde edilmiřtir. Elde edilen veriler zerinde analizleri gerekleřtirebilmek iin eř zamanlı verilerin belirlenmesi amacıyla veri setinden zaman bileřenini okuyan ve eřleřtiren bir algoritma yazılmıř ve kullanılmıřtır.

Kpr tařıyıcı plakası altında tesis edilen hedeflerin resim koordinatlarının pikselaltı dođrulukta belirlenmesi iin grnt eřleřtirme algoritmaları kullanılmıřtır. Her bir hedef iin tek tek piksel koordinatı belirlemek yerine tm hedeflerin tek bir eřleřtirme ile belirlenmesi hedeflenmiřtir. Bu amala ana grnt zerinde hedeflerin yaklařık konumları belirlenmiř ve her bir hedef iin arama alanları; aranan pikselin piksel boyutlarının karesi olacak řekilde arama penceleri belirlenmiřtir.

Elde edilen piksel koordinatlarının resim koordinatlarına dnltrlmesi, resim koordinatları kullanarak cisim koordinatlarının hesaplanması fotogrametrik deđerlendirme iřlem adımları ile hesaplanmıřtır. Arařtırma; yer deđiřikliklerinin hesaplanması ve grselleřtirilmesi ile sonulandırılmıřtır.

1. INTRODUCTION

Like each engineering structure also bridges are subject to the natural aging process. They are exposed to strong loads, constantly changing load conditions, changing weather conditions as well as associated material stressing. Regular control monitoring for the material fatigue as well as of appearing damage is essential for the early recognition. A late assessment of damages increased not only the danger potential, also raises the costs of reorganization strongly. The renewal need of existing buildings represents a heavy mortgage for the future of a society. The solution of this problem is an important task for the researchers and the building industry together to develop a suitable monitoring from planning to the execution.

1.1 Aim of the Study

In the context of this research, new methods and procedures for the determination of the current condition of the bridge construction would be developed and thus for the early recognition and documentation of arising damage was going to be displayed. For the suspension bridges; the shifts of individual building bodies; main suspension cable, carriageway pavement and Pylons, would be determined. The received shifts serve for the determination of the static and dynamic stresses of the bridge sections. Shifts of the individual construction units are important indicators of the structural behavior of the bridge. Therefore, the demands of the bridge sections can be computed from the shifts with the help of finite elements method and can be compared with the indicated values. A further supplementing method to the procedures described above is the photogrammetric measurement of the roadway, even without reflecting goals. Therefore, the production of a combined measuring and logging system could be carried out for the on-line monitoring of the bridge without problems.

1.2 Structure of the Thesis

In this section a brief introduction and aim of the study is defined. The section summarizes the causes and consequences of bridge deformation and monitoring and related literature. The third section addresses the proposed design, by the means of the network design and simulation, calibration, image acquisition and synchronization, photogrammetric evaluation procedure and spatial displacement analysis. The pre and onsite tests and measurements were explained in the fourth section. The computational results were discussed and recommendations for future works were summarized in the last section.

2. STATE OF ART

2.1 Deformation Monitoring of Engineering Structures

One of the most important objectives of geodetic and photogrammetric measurements is analysing of deformation occurring depending on time, affected factors and strengths on natural and artificial (man-made) objects (Bogatin et al., 2008).

The basic process steps to be followed for monitoring deformations of engineering structures can be expressed as follows:

- Determination of the performance (state) of the structure,
- Positioning accuracy requirement and selection of the method,
- Type and number of measurements
- Tools and equipment selection,
- Measuring and data collection,
- Evaluation of data and analysis,
- Determination of the behavior of the deformations within the time, location and frequency,
- Modelling,
- Reporting.

Geodetic and non-geodetic methods are used in conjunction during the monitoring of the deformation of the engineering structures such as dams, bridges and tunnels. In geodetic method, measurements carried out at appropriate intervals by creating networks, and sometimes it is possible to make continuous monitoring with automated measurement and positioning systems (Kalkan and Alkan, 2005).

Like all engineering structures; bridges are affected by the aging process. In addition, they are exposed to intensive and/or variable loads, variable weather conditions and

material fatigue depending on land or rail line that they are in conjunction with. The factors mentioned above are the main components that impact the bridge deformations.

As a result of the carried-out studies and their outcomes; regular inspection and monitoring was proved to provide significant gains on detecting fatigue and deformations that may occur in structural elements. The importance of the early monitoring and identifying studies once again arise with the consideration of repair, maintenance and even the reconstruction costs. Both being the main links of the transportation network and their economic importance; bridge deformations should be monitored continuously.

Displacements may occur on the structural elements of the suspended bridges such as main carrier cables, road surface and pylons. In order to determine these displacements (movement/changes); traditional geodetic methods, total station surveying, Self-levelling, Hydrostatic levelling, deviation measurements, EDM, laser surveying, photogrammetric methods and satellite-based methods are used. The static and dynamic stresses of the bridge components and the behavior of the structural elements of the bridge are determined with the obtained data.

2.2 Deformation Analysis Applications of Close Range Photogrammetry

A very first photogrammetric bridge monitoring project, including a condition survey and vertical deflection measurement, was carried out by Bales and Hilton in 1985. The bridge has a 3-span continuous structure with a total length of 139 m. The length of the centre span was measured as 51 m. The camera was positioned at three locations under mid-span facing up at a distance of about 10.8 m. The average difference between photogrammetric measurements and level readings was approximately 3 mm (Bales and Hilton, 1985).

Kim (1989) performed a long-term deformation monitoring of a 526 m long highway bridge using photogrammetry. The project utilized a camera with a 150 mm lens. The distance between the bridge and the camera was 122 m. Images were recorded on conventional 230 x 230 mm film and were analysed using a program developed specifically for the project. It was concluded that the precision of the deformation

measurement using photogrammetry was within ± 14 mm in the length and height directions, and ± 30 mm in the width direction (Kim, 1989).

Fraser and Riedel (2000), performed a study on the monitoring of thermal deformations of steel beams. The temperature variation of the steel beams ranged from 1100 LC down to 50 LC, and the measurement rate was one set every 15 s. In order to collect approximately 70–80 sets of measurements in about 2 h, a highly automated, on-line data processing system was used. Two groups of targets were utilized. Group 1 had about 10 to 15 targets, and was used to monitor the deformation of the beam; group 2 had about 30 targets that were placed on the wall behind the beams and stayed stationary during the entire test, serving as reference points. The average camera-to-object distance for the outer cameras was 9.6 m, and 6.7 m for the centre camera. An Australis system was used for the off-line photogrammetric analysis, which was modified for the on-line process of real time measurement. The coordinate changes of the targets on the steel beam were recorded continuously over time. The final RMS value of coordinate residuals in approximately 800 point measurements averaged 1.6 lm (close to 0.2 pixels), which yielded an accuracy in the object space of 0.7–1.3 mm (Fraser and Riedel, 2000).

Sewall Company applied digital close-range photogrammetry to measure the geometry of the 622 m long Waldo-Hancock Cable Suspension Bridge between Prospect and Verona, Maine. The bridge was built in 1931 and had shown serious deterioration both in its superstructure and deck. The bridge dimensions measured by photogrammetry were used in the rehabilitation planning of the bridge. Control points were placed at the approaches to the bridge and surveyed using a total station, along with real-time kinematic (RTK) GPS methods. Images were acquired from a helicopter. From photogrammetric analysis, Sewall provided information on bridge and cable geometry for further structural analysis. The measurements included the elevation and offset of cables, trusses, piers, the main tower, and cable bents. The accuracy of measurement for critical dimensions of the bridge was comparable to that of a conventional survey. The standard deviation of the photogrammetric measurements was 3 mm over a length of 213 m of a bridge section, and 15.9 mm over the total length of the bridge. Compared to traditional surveying methods, close-range photogrammetry proved to be more efficient. Measurements accomplished in less than three days in the field would have taken 10 days for a conventional survey,

and images were acquired without physically accessing each measurement point. The whole process was non-intrusive, and only created minimal impact on traffic flow (Johnson, 2001).

Leitch (2002) and Jauregui et al. (2003) conducted a comprehensive study on bridge deflection measurement using close-range photogrammetry. Studies were performed on a laboratory steel beam and on two field bridges. The first bridge tested was a single-span, prestressed concrete bridge with a length of 32.2 m. The second was a simple-supported steel girder bridge, under truck loading and having 7-spans. In the experiments of the first bridge, photogrammetric measurements of the initial camber were compared with level rod readings. The maximum deviation of the two measurements was within ± 17 mm for four of the girders, and 28 mm for the remaining girder (Leitch, 2002). For the second experiment; the photogrammetric measurement results were compared with those obtained from finite element analysis, level rod readings, and curvature-based measurements derived from strain gages. The maximum deflection was about 8 mm. The differences in deflection measurements from photogrammetry, curvature, and the level rod were within 0.5–1.5 mm for all girders at the mid-span (Jauregui et al., 2003).

Hegger et al. (2004) reported a test on pre- and post-cracking shear behavior of prestressed concrete beams using laser-interferometry and close-range photogrammetry. Laser-interferometry was used to measure the pre-cracking behavior, while close-range photogrammetry was applied to measure the post-cracking shear behavior. The beam web was marked with black measuring dots at a spacing of 25 mm for photogrammetry measurement. Photos were taken at nine stations from two elevations around the marked area for each loading step. Calibrated rods were placed at the top and bottom of the beam for setting scale. The accuracy of the 3D coordinates of the measured points was 0.02 mm, which accurately determined the crack locations and openings. From the measurement of cracks and monitoring their development, the shear transferred across the cracks by shear friction was estimated (Hegger et al., 2004).

Zogg and Ingensand (2008) present a deformation monitoring application with Terrestrial Laser Scanning for an 1116 m length viaduct and verified their results with precise levelling (Zogg and Ingensand, 2008).

Koo and et al. (2010; 2013) presents a structural health monitoring system using an automated Total Positioning System and its application to a 3-span suspension bridge. Fifteen reflectors were installed on the bridge deck, on top and wall of towers and on top of side towers, monitored for a period of three months to measure the longitudinal, vertical and lateral movements of the bridge (Koo and et al., 2010; 2013).

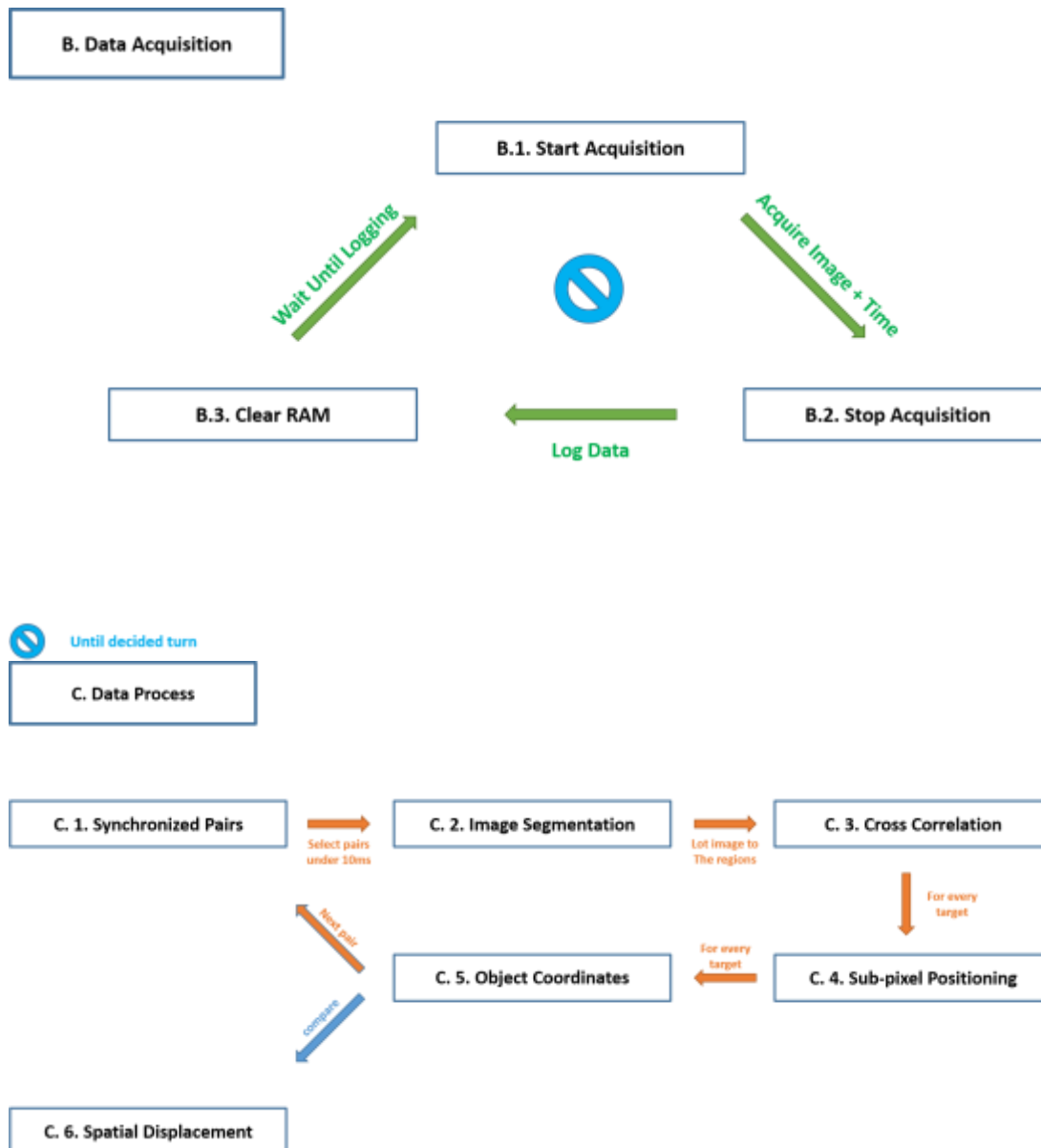


Figure 3.1 (continued) : Flowchart diagram.

3.1.1 Network design and simulation

In order to determine the camera that will be used for the studies some previous investigations were carried out for various industrial cameras. Firstly a field of view test was carried out. For this purpose; a field of view pyramid was created in CAD design according to the known camera parameters (sensor size and focal length). This pyramid was manually rotated to determine whether the target points are located inside. To automate this methodology an algorithm based on point-plane relationship was developed. Since the pyramid consists of four planes intersect at the projection centre and each of these planes divides the object space in two pieces (positive/negative); it is possible to determine the position of the target point

Unknown sensor size: The algorithm calculates the required sensor size to hold all target points (3.1). While f refers to focal length, ε refers to limit angle (limit angle can be define if user wants to have a wider view) and SW and SE refers to sensor width and height respectively, following equations calculates the required sensor size:

$$SW = 2 * f * \tan\left(\frac{\alpha + \varepsilon}{2}\right) \quad SH = 2 * f * \tan\left(\frac{\beta + \varepsilon}{2}\right) \quad (3.1)$$

Known sensor size: According to the above formula, angles (α and β) provided by the sensor size can be calculated.

For the further steps algorithm calculate an average distance from the projection centre to the angularly mean (for each plane pairs) of the target points and calculates the four corner of the pyramid. Consequently plane equations acquired and algorithm results the relation of the target points and planes in simplified notation (1 for all positive values and -1 for all negative values) (Table 3.1).

Table 3.1 : Example result of the algorithm.

Target Points	D1	D3	D1&D3	D2	D4	D2&D4	Field of View Pyramid
1	1	-1	0	1	-1	0	0
2	-1	-1	-2	1	-1	0	-2
3	1	-1	0	1	-1	0	0
4	1	-1	0	1	1	2	2
5	1	-1	0	1	-1	0	0
6	1	-1	0	1	-1	0	0

In the above table column 2, 3, 5 and 6 show the relation between point and plane, column 4 and 7 shows the situation between the opposite planes and column 8 show the position of the point according to pyramid.

According to above table given as an example:

- Target points 1, 3, 5 and 5 are in the field of view pyramid,
- Target point 2 stands on the left side of the planes 1 and 3, stands between the planes 2 and 4, hence out of the pyramid,
- Target point 4 stands on the stands between the planes 1 and 3, stands above the planes 2 and 4, hence out of the pyramid.

The proposed algorithm was generalized for independent solutions for more than one camera (Figure 3.4).

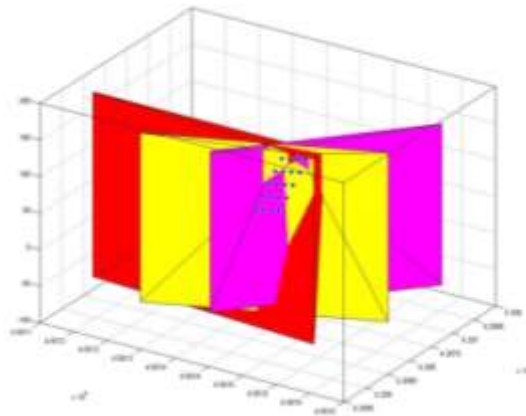


Figure 3.4 : Diagram for 3 cameras.

A second test, introduced by Parian, was carried out to determine the theoretical standard deviations for the target points according to number of cameras and focal length (Amiri Parian et al., 2007). In the following table a camera with a 1280 pixel x 1024 pixel image size and 0.00465 mm pixel pitch was examined with several focal lengths (Table 3.2).

Table 3.2 : Standard deviations according to number of cameras.

<u>Nof. Cameras</u>	<u>c (mm)</u>	<u>StdDev. (X, Y, Z) (mm)</u>
4	6	±100.5 (87.4 49.4 4.9)
4	8	± 95.8 (83.0 47.5 5.0)
4	10	± 78.3 (66.5 41.2 3.1)
3	8	±119.3 (105.7 54.9 4.7)
3	10	±110.3 (90.0 63.6 3.5)
2	6	±147.3 (120.1 85.2 6.7)

Above table indicates 2 cameras don't provide enough accuracy and there is an only 1 cm difference between 3 and 4 cameras. Therefore further tests were carried out for 3 cameras. The result for the selected camera and lens result is given in the following table (Table 3.3).

Table 3.3 : Standard deviations according to focal length.

<u>Nof. Cameras</u>	<u>c (mm)</u>	<u>StdDev. (X, Y, Z) (mm)</u>
3	16	± 76.1 (65.4 38.6 2.9)
3	18	± 53.3 (46.0 26.9 2.5)

3.1.2 Video camera and camera calibration

According to the results of the previously explained tests three Basler A402k cameras (Figure 3.5, Table 3.4) with Carl Zeiss SLR Lens Distagon T* 3,5/18 were decided to use for this study.

The A400 series was developed with the goal of offering a high performance camera to meet the most stringent requirements in terms of resolution, speed and image quality.



Figure 3.5 : Basler 402k.

The standard CameraLink interface used on the A400 family makes these cameras compatible with frame grabbers produced by many different vendors. A frame grabber is an electronic device that captures individual, digital still frames from an analogue video signal or a digital video stream. It is usually employed as a component of a computer vision system, in which video frames are captured in digital form and then displayed, stored or transmitted in raw or compressed digital form. Historically, frame grabbers were the predominant way to interface cameras to personal computers. This has substantially changed in recent years as direct camera connections via USB, Ethernet and IEEE 1394 ("FireWire") interfaces have become prevalent. Two Matrox Solios eV-CL framegrabber were used during the studies that supports the full-range of Camera Link interfaces (dual-Base, single Medium/Full, 10-tap and PoCL) and offloads typical pixel pre-processing tasks.

Carl Zeiss SLR Lens Distagon T* 3,5/18 (**3.5**) was selected to use since its image performance over the entire image field.

Table 3.4 : Camera specifications.

Basler A402k	
Sensor Size (H x V pixels)	2352 x 1726
Sensor Type	Progressive Scan CMOS
Optical Size	1 1/4"
Camera Link Clock	50 MHz
Max. Frame Rate (at full resolution)	24 fps
Color / Mono	Mono
Video Output Type	Camera Link (Base)
Video Output Format	2 taps, 8 bits/10 bits
Synchronization	Via external trigger or free-run
Exposure Control	Level-controlled, or programmable
Power Requirements	12 VDC ($\pm 10\%$); Max. 8.0 W
Lens Mount	F-mount
Housing Size (L x W x H)	42 mm x 90 mm x 90 mm (without lens adapter)
Weight	Max. 605 g
Conformity	CE, FCC
Housing Temperature	Up to 50°C

Table 3.5 : Lens specifications.

Basler A402k	
Focal length	18 mm
Aperture range	f/3.5 – f/22 (1/ 2 stop intervals)
Number of elements / groups	13.Kas
Focusing range	0.3 m (0.98 ft) –
Angular field (diag. / horiz. / vert.)	99 / 90 / 67 °
Coverage at close range	44 x 29 cm (1.7 x 1.1")
Image ratio at close range	01:12
Filter-thread	M 82 x 0.75
Length (with caps)	84 - 85 mm (3.3")
Diameter	87 mm (3.4")
Weight	470 - 510 g (16 - 18 oz.)
Camera mounts	ZE (EF bayonet) ZF.2 (F bayonet with CPU) ZF (F bayonet) ZK (K bayonet)
Scope of delivery Lens Shade included	Lens Shade included

With the calibration process focal length, principal point coordinates and image coordinate corrections to meet the different deviations from the co-linearity condition can be determined. The calculation of these parameters is required to obtain high-precision measurement results. There are four main sources of the deviations for the ideal geometry of co-linearity condition. These are: systematic radial distortion, tangential distortion, non-planarity image plane and the image distortion on plane. Translation from the theoretical position of any image point is the sum of the effects of each of these sources (Fraser, 1997, Habib and Morgan, 2003). Furthermore image coordinate corrections can be expressed (3.2):

$$\Delta x = \Delta x_r + \Delta x_d + \Delta x_u + \Delta x_f \quad \Delta y = \Delta y_r + \Delta y_d + \Delta y_u + \Delta y_f \quad (3.2)$$

In these equations, r refers to radial distortion, d refers to tangential distortion, u refers to non-planarity and f refers to image distortion on plane.

In analytical photogrammetry, radial lens distortion is mathematically expressed by a polynomial function (3.3) while k1, k2 and k3 refers to coefficient of radial distortions and r refers to radial distance:

$$\Delta r = k1r^3 + k2r^5 + k3r^7 \quad (3.3)$$

Non-alignment of the lens components also cause radial and tangential distortions that could expressed with the given formula (3.4):

$$\begin{aligned} \Delta x_d &= p1.(r^2 + 2.\bar{x}^2) + 2.p2.\bar{x}.\bar{y} \\ \Delta y_d &= 2.p1.\bar{x}.\bar{y} + p2.(r^2 + 2.\bar{y}^2) \end{aligned} \quad (3.4)$$

Non-planarity image plane and the image distortion on plane can be ignored according their effects on image point coordinates.

The calibration of the cameras has been carried out by using two photogrammetric software by using the image of the test field (Figure 3.6) established at the Institute of Geodesy and Photogrammetry at ETH, Zurich.



Figure 3.6 : Calibration test field.

The results of the calibration process is given in the below table (Table 3.6).

Table 3.6 : Calibration results.

BAAP	Camera 1		Camera 2		Camera 3	
c (mm)	18.5996	0.0004	18.5831	0.0004	18.5946	0.0004
x0 (mm)	0.1426	0.0008	0.1000	0.0008	0.0741	0.0007
y0 (mm)	0.1977	0.0006	-0.1414	0.0006	0.1357	0.0006
K1	-0.00026605	0.00000152	-0.00026724	0.00000149	-0.00025754	0.00000142
K2	0.00000112	0.00000006	0.00000116	0.00000005	0.00000116	0.00000005
K3	0.00000000	0.00000000	0.00000000	0.00000000	-0.00000001	0.00000000
P1	0.00000219	0.00000086	-0.00000938	0.00000084	0.00000259	0.00000082
P2	-0.00000296	0.00000068	-0.00001463	0.00000065	-0.00001683	0.00000065
B1	-0.00007518	0.00000415	0.00008391	0.00000399	0.00004685	0.00000390
B2	-0.00002672	0.00000206	0.00003797	0.00000198	-0.00005043	0.00000193

Pictran	Camera 1		Camera 2		Camera 3	
c (mm)	18.5932	0.0027	18.5812	0.0001	18.5926	0.0006
x0 (mm)	0.1460	0.0018	0.1000	0.0001	0.0738	0.0005
y0 (mm)	0.2026	0.0032	-0.1414	0.0001	0.1361	0.0008
A1	-0.00025727	0.00000277	-0.00025777	0.00000014	-0.00024219	0.00000063
A2	0.00000090	0.00000005	0.00000093	0.00000000	0.00000073	0.00000001
A3	0.00004126	0.00000963	-0.00004149	0.00000043	-0.00002448	0.00000232
A4	-0.00004013	0.00000969	0.00003735	0.00000043	-0.00005121	0.00000233
A5	0.00000229	0.00000259	-0.00001409	0.00000012	-0.00001655	0.00000061
A6	0.00000349	0.00000290	-0.00000884	0.00000013	0.00000260	0.00000068

3.1.3 Video-tacheometers

Video-tacheometers or IATS represent a new kind of Total Stations. They offer the user (metrology expert) an image capturing system (CCD/CMOS camera) in addition to a polar 3D point measurement system. The system is capable of capturing panoramic image mosaics through camera rotation – with appropriate calibration, these images are accurately geo-referenced and oriented, and can be immediately used for direction measurements with no need for object control points or further photogrammetric orientation processes.

The development of IATS has to be seen in combination with research work done in the field of reflectorless distance measurement systems (Gottwald, 1987, Katowski, 1989). The latest developments in the area of IATS are done by Leica Geosystems (Walser, 2004, Leica Geosystems 2012), the Ruhr-Universität Bochum (Scherer, 2004), the i-MeaS project at Vienna University of Technology (Reiterer et al., 2010), the alpEWAS and DE-MONTES project at the Technische Universität München (Wasmeier, 2009, Wagner, 2012), Topcon (Topcon 2012), and Trimble (Trimble 2012).

This development is already progressed so far that four instrument manufacturer have added IATS to their product line (Figure 3.7).



Figure 3.7 : Current commercial available IATS.

All devices have an integrated wide-angle camera with fixed focus next to the telescope. Only the instrument of Topcon has an additional image sensor, which reproduces the current view of the telescope including the variable focus. Only thus

the entire accuracy potential of an image-imaging total station can be used. Interesting is the design of Pentax, wherein the camera, and a small screen is implemented as a component above half of the telescope. With this modular design, the base total station to be rebuilt R400 into an imaging instrument.

The image function is currently only used as a supportive service to the normal measurement task of a total station. In detail these are:

- Documentation,
- Overlay of live and measurement, planning, or hand sketch data
- Target and range selection in the image,
- Georeferenced Photo Texture (scan)
- Simple edges and point detection as aids.

Table 3.7 : Comparison of the current commercial available IATS.

	Trimble VX/S8	Topcon IS/-3	Pentax Visio	Leica Viva
Camera	wide angle	wide angle + coaxial	wide angle	wide angle
Resolution	2048 x 1536	1280 x 1024	2048 x 1536	2560 x 1920
Field of view	16,5° x 12,3°	28° x 22° 1° x 1°	8,8° x 8,8°	15,5° x 11,7°
Focus	3m - ∞	2m - ∞	20m - ∞	2m - ∞
Frame rate	5 Hz	10 Hz	-	20 Hz
Zoom	up to 8x digital	up to 4x digital 30x optic	up to 3x digital	up to 4x digital

The live video with frame rates listed in the above table (Table 3.7) is currently exclusively used on the instrument or remote control screen. Only single images can be saved to the internal memory of the instrument or to memory cards.

3.2 Image Acquisition and Synchronization

Image acquisition step was carried out by generating a Matlab code (Figure 3.8). For this purpose a camera file, also known as a device configuration file was created by using camera configuration toolbox supported by the camera distributor. This camera file introduces the basics of the camera to Matlab such as: Camera name, running

mode, maximum resolution, number of bits, maximum frames per seconds and cable connections.

```
function fun1(~)
d1=800; d11=2352; nobsl=24;
vid101=videoinput('matrox', 1,'Devil1.dcf');
triggerconfig(vid101, 'Manual');
set(vid101,'TriggerRepeat',inf);
set(vid101,'FramesPerTrigger',1);
set(vid101,'TriggerFrameDelay',0);
set(vid101,'ROIPosition', [0 500 d11 d1]);
start(vid101)
frameNumber1=0;
while (frameNumber1 <= nobsl)
    frameNumber1 = frameNumber1 + 1;
    trigger(vid101);
    wait(vid101,2,'logging');
end

[data1, ~, c1] =getdata(vid101,nobsl,'uint8','numeric');
cv1=zeros(nobsl,1); cv11=zeros(nobsl,1);
datav1=zeros(d1,d11,nobsl);

for i=1:nobsl
    cv1(i,1)=c1(i,1).AbsTime(6);
    cv11(i,1)=c1(i,1).AbsTime(5);
    datav1(:,i)=data1(:,i,1,i);
end
parsave1(sprintf('v101o%d', lo2, lo1), datav1, cv1, cv11);
stop(vid101);
delete(vid101);
end
```

Figure 3.8 : Image acquisition code.

The other required parameters should be determined by the algorithm:

- Camera port: Since some framegrabbers has more than one port, user should verify which camera is on which port using more than one camera at the same time.
- Trigger configuration: The normal setting is immediate triggering that means acquisition starts with the acquisition camera starts. Simultaneous image acquisition needs to trigger all cameras concurrently.
- Trigger repetition: Allows user to determine number of total frame grabbed during the acquisition.
- Frames per trigger: Allows user to determine how many frames will be grabbed during one trigger.

- ROIPosition: Allows user to select region of interest.
- Logging: Manually system log the grabbed data to the memory. User can select to log to disk as a VideoWriter file.
- Start/Stop: Allow user to start/stop image acquisition period.
- Delete: Computer memory conditions should be cleaned, since system log the grabbed data to the memory
- Fps: Determines how many frames per second will be grabbed during the acquisition

For image synchronization; a “for” loop was created that provides starting image acquisition at the same time for each cameras. In addition; advantage of parallel computing was used by the Matlab pools (Figure 3.9).

```
function ozgur3
    data01 = clock; data02 = clock;
    funList = {@fun1, @fun2};
    dataList = {data01, data02};

    matlabpool open 2

    for lo2=1:20
        for lo1=1:20
            spmd
                labBarrier
                funList{labindex}{dataList{labindex}}
            end
        end
    end

    ...
    function fun1(~)
    ...
    end
    function fun2(~)
    ...
    end

    matlabpool close
end
```

Figure 3.9 : Part of the written code.

3.3 Automatic Target Recognition

Automatic image matching algorithms are widely used to measure the coordinates of the targets in images.

Area-based image matching by least-squares: Is based on searching homologue of the reference image one or more of the image. Since least squares equations are used it provides high accuracy. It requires approximate search area. It is recommended not to use image pairs with more than 30 degrees rotation and more than 25 percent of the scale factor.

Feature-based image matching: Based on the principle of occurring in the same way for a specifically particular point or line on a template image and search images. Therefore it is generally used to determine lines, edges, corners, and so on.

Image matching of multiple photographs with geometric constrains: Can be determined as matching by using geometric rules and constraints. Therefore it provides to determine incorrect matching. Generally used for dead zones and shaded areas.

Relational matching: Generally used for understanding and interpreting images and determining certain structures and objects with their spatial topologies. This matching does not aim a precise geometric matching.

Shape from shading: Use to determine the shape of brightened objects depending on their shadows on the images. This method is not preferred to use in photogrammetric studies due to its lower accuracy.

3.3.1 Image segmentation

In computer vision, image segmentation is the process of partitioning a digital image into multiple segments. The goal of segmentation is to simplify and/or change the representation of an image into something that is more meaningful and easier to analyse. Image segmentation is typically used to locate objects and boundaries (lines, curves, etc.) in images. More precisely, image segmentation is the process of assigning a label to every pixel in an image such that pixels with the same label share certain visual characteristics. The result of image segmentation is a set of segments

that collectively cover the entire image, or a set of contours extracted from the image.

3.3.2 Cross correlation

Matching interest points in two uncalibrated images is a fundamental problem in computer vision. Normalized cross correlation is widely used in many applications that require matching parts of the images. The implementation closely follows following formula (3.5):

$$\gamma(u, v) = \frac{\sum_{x,y} [f(x, y) - \bar{f}_{u,v}] [t(x-u, y-v) - \bar{t}]}{\left\{ \sum_{x,y} [f(x, y) - \bar{f}_{u,v}]^2 \cdot \sum_{x,y} [t(x-u, y-v) - \bar{t}]^2 \right\}^{0.5}} \quad (3.5)$$

Where f is the image, \bar{t} is the mean of the template and $\bar{f}_{u,v}$ is the mean of $f(x,y)$ in the region under the template.

3.3.3 Sub-pixel positioning

Pixel-level accuracy might be satisfactory depending on the spatial resolution of the imagery available and the type of process being investigated. Improving NCC precision, however, improves displacement accuracy two folds: by reducing the image co-registration error and by improving the matching accuracy directly. To achieve sub-pixel precision in NCC, two approaches can be used. The first option is to resample the image intensity to a higher spatial resolution through interpolation. The second option is to interpolate the cross-correlation surface after the matching process to a higher spatial resolution in order to locate the correlation peak with sub-pixel precision. There are also area-based spatial domain methods that are intrinsically capable of sub-pixel precision such as the least squares matching, which is more often used in stereoscopic Digital Elevation Model generation and image registration. Least square matching is known for its capability to deal with scaling and rotation (Debellia-Gilo and Käab, 2011).

In this study interpolation, according to the NCC results of neighbour pixels, a second degree function was implemented to achieve sub-pixel positions of the targets. In this approach the previous, related and next pixels in x and y direction are put in place in the equation to calculate the coefficients of the function.

3.4 Synchronous Matching of Image Pairs

Since the data is provided from more than one sensor, there would be time differences between acquisition times. Therefore; time component of the data acts an important role and should be recorded with image acquisition. An algorithm that matches image pairs according to their acquisition time was developed and used in this study.

3.5 Computation of the Object Coordinates of the Targets

Computation of the object coordinates follows the general orientation process photogrammetric evaluation. The automated inner orientation step calculates the corrections of the image coordinates according to the calibration parameters. In digital photogrammetry, the last equation for the description of the mathematical model is an affine transformation between the metric coordinate system on image plane and pixel coordinate system (Dappuzo, 2003, Remondio, 2004).

Furthermore, for calculating the exact coordinates of the target points, the mathematical formulas, based on co-linearity condition of photogrammetry, that describe the relationship between image and object coordinates should be used. Since these formulas are not linear, differential equations should be obtained by linearization. Differential equations can be solved iteratively by calculating the corrections according to least square adjustment. Definite outer orientation parameters and object coordinates of the targets can be calculated by applying the calculated corrections to the previous values. This iterative approach requires preliminary values and these values acquired from field measurements. A Matlab code was written and used for these photogrammetric evaluation steps.

3.6 Spatial Displacement Analysis

Under the action of forces (body forces or surface forces) a deformable body undergoes changes in its shape and position. These changes occur either gradually or suddenly. The determination and interpretation of the changes are the main goal of deformation surveys. In this chapter a brief review of the basic deformation parameters is first given; then monitoring methods, techniques and their achievable

accuracies are summarized; finally, the functional relations between the deformation parameters and the observables are developed (Yong-Qi, 1983).

Spatial displacements of targets were calculated from coordinate's differences between each epoch and origin. Also, instant displacement inspected between consecutive epochs. All these displacements were visualized in Matlab by using related diagrams.

4. APPLICATION

For the first indoor test, a pendulum established at the laboratory of Geomatics Engineering Department of ITU in order to observe its oscillation.

For the second indoor test, it was aimed to determine the displacements of steel reinforcements, embedded into concrete by using chemical anchorages, while applying axial pulling loads by means of monitoring and photogrammetric evaluation. The test field was established in the Construction Materials Laboratory of Istanbul Technical University. Two steel reinforcements with 16 mm diameter and two with 20 mm diameter were observed during the experiment.

For the main object the Second Bosphorus Bridge, which is a modern type of suspension bridge, was monitored, since it lies on the main arteries of the Turkish transportation net. A 2-days image acquisition campaign was performed in the field. Three still video cameras were used to monitor the movement of the bridge platform using the photogrammetric technique with a 2352 x 800 pixels field of view and 12 fps image acquisition frequency.

4.1 Preliminary Laboratory Experiments and Applications

4.1.1 Laboratory condition oscillation test

An in-door test was performed using a pendulum setup which was established at the photogrammetry laboratory of the Geomatics Engineering Department of Istanbul Technical University. The oscillation of the pendulum (Figure 4.1) was monitored by the three cameras with an image acquisition frequency of 24 fps. Only an area of interest of 1200 x 880 pixels over the full image format was recorded thanks to the windowing capability of the CMOS sensor. The in-door pendulum test gave useful information about the synchronization error and the point positioning error prior to the out-door tests.

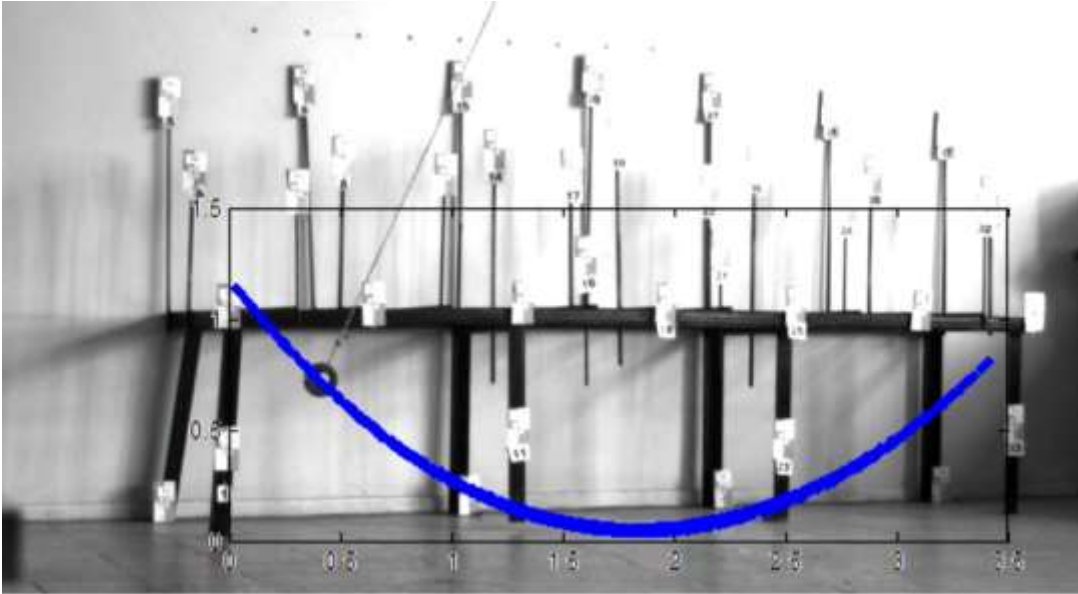


Figure 4.1 : The pendulum setup.

4.1.2 Test on pull-out deformations of bonded metal anchors embedded in concrete

In strengthening applications such as, column jacketing, and the addition of new shear walls to the existing system on frame axes by replacing brick walls, anchorages are widely used for connecting these new vertical members to the existing structure in order to transfer the loads to the foundations and, to secure the combined resistance of existing and strengthening members. Chemically bonded anchors, which can be described as a rod attached to a pre-drilled hole with construction chemicals, are frequently used in rehabilitation and strengthening applications due to the ease of their applications procedures (Kaya, 2007).

Chemical anchors are the simplest methods for achieving the adherence between existing and new constructed reinforced concrete members. However, strength of these anchors can show great differences with respect to the type of chemical, cleanliness of anchor hole and compressive strength of concrete (Yilmaz et al., 2010).

Deformation measurement during laboratory testing on construction materials aims at determining the intrinsic characteristics of the considered object. The examination of the deformation and the knowledge of the applied load (e.g., a mechanical or thermal load) allow the analysis of the mathematical model that describes the behavior of a construction element (Barazzetti and Scaioni, 2010).

According to standard “Products and systems for the protection and repair of concrete”; coded EN 1881, deformations corresponding to the axial tensile loads should be measured. In addition to this; in the standard “Products and systems for the protection and repair of concrete structures, Definitions, requirements, quality control and evaluation of conformity, Anchoring of reinforcing steel bar”, coded EN 1504-6, 0.6 mm is given as the maximum value of deformation for a steel reinforcements which has 16 mm diameter, under 75 kN load which is applied during the test method defined in EN 1881. Also; load at loss of adhesion can be calculated from load - deformation graphs according to guideline published by European Technology Assessment Group.

In this step of the study; it is aimed to determine the displacements of steel reinforcements, embedded into concrete by using chemical anchorages, while applying axial pulling loads by means of monitoring and photogrammetric evaluation.

Knowledge of structural behavior of anchorage under the applied axial tension is essential for safe design. In the retrofitting applications; compatibility of the additional elements to the supporting system of the existing structure and providing a safe load transfer depends on the performance of the implemented anchors. Anchorages transfer the tensile loads throughout the cohesive depth of the anchorage. Adherence can be called as the shear stresses that provide bonding between reinforcements and epoxy or concrete and epoxy. Components of adherence in chemical anchorages can be considered as; friction force, chemical bond strength and mechanical gear force occurred as the results of ribs on the anchorage. During the pull-out tests; various failure modes may be observed depending on the concrete class, type of chemical anchorage, geometry of the anchorage, durability and depth of the anchorage (Figure 4.2).

Behavior of anchors; under the influence of the axial tensile load, can be classified in five categories:

1. Flowing/Rupturing of Anchorage reinforcement: This situation is the preferred one for the designer.
2. Pull out of Anchorage reinforcement: Chemical anchors begin to pull out along the anchoring depth, with the ending of the adhesion strength.

3. Conic Rupturing of the concrete: Provided tensile stress exceeds the tensile strength of concrete; conical failure of the anchored concrete may take place.
4. Simultaneous Pull-out and Conic Rupturing
5. Splitting of the concrete: Where the depth of the base element is shallow or planting the anchorage near the edge may cause splitting of the concrete.

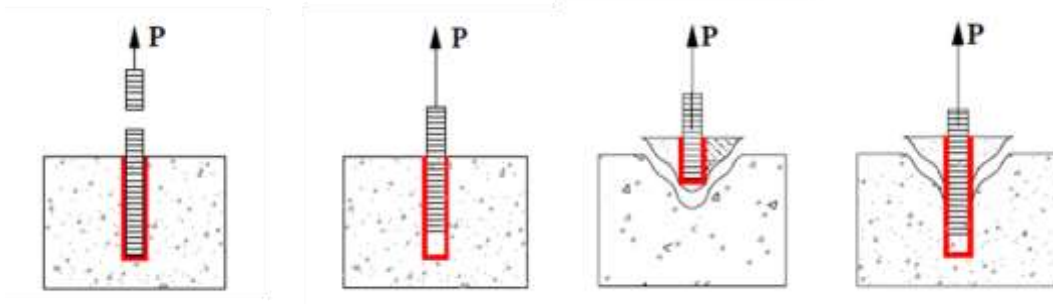


Figure 4.2 : Mode of failures of Anchorages (ACI 355, 1991).

The most widely adopted tools are linear-variable-differential-transformers (LVDTs) and strain gauges, which provide the magnitude of the displacement with the investigation of the changes of electrical resistance due to a load. These tools are considered proven techniques, with an accuracy of $\pm 1 \mu\text{m}$ or even less, and they give real-time data. On the other hand, they only provide 1D measurements limited to the area in which the sensor is fixed. In addition, a connection with a control unit is necessary and after destructive tests these kinds of sensors can be damaged. Thus, LVDTs or strain gauges are not a convenient choice in the case of extensive analysis on the whole body, in which a great number of 3D points with a good spatial distribution must be measured (Barazzetti and Scaioni, 2010).

In these cases, techniques of digital photogrammetry depict a valuable option for the design of powerful and flexible measurement tools. The use of photogrammetry in material testing experiments will generally allow for the simultaneous measurement of deformation or displacements at an almost arbitrary number of locations over the camera's field of view. Data processing can be highly automated and fast, allowing for real-time monitoring at the camera imaging rate (Maas and Niederöst, 1997; Albert et al., 2002; Maas and Hempel, 2006).

The test field was established in the Construction Materials Laboratory of Istanbul Technical University. Two steel reinforcements with 16 mm diameter and two with 20 mm diameter were observed during the experiment. All of the reinforcements were all embedded in the concrete with a depth of ten times of their diameters within a C30 grade concrete (Figure 4.3).



Figure 4.3 : Test field.

The process of measurement can be defined as following:

1. A few randomly distributed ground controls points were measured with an accurate TPS.
2. 3 artificial points were established on the reinforcement.
3. Images were recorded from camera stations under empty load. The 3D coordinates of targets on the steel reinforcement were computed. The result is defined as the basic stage.
4. Increase the pressure continuously by 10 bars on the steel reinforcements and wait till the deformation is stable.
5. Images were grabbed.
6. Steps 4-5 were repeated until the reinforcements get free of the concrete.

During the experiments, displacements were occurred under 130, 128, 184 and 189 kN loads for reinforcements with 16 and 20 mm diameter, respectively. Therefore 31 images pairs for the reinforcements 16 mm diameter and 45 images pairs for the 20 mm pairs were grabbed.

Post-processing evaluation of image pairs for reinforcements carried-out by using photogrammetric evaluation software. The acquired displacements (Table 4.1, Table 4.2) and displacement-load curves (Figure 4.4) are given. Since the coefficient of the pressure-load equation of the hydraulic cylinder is $k=41.794$, loads were calculated with:

$$F(kN) = \frac{P(bar) * k * g}{1000} \quad (4.1)$$

Table 4.1 : Observed displacements for the 16 mm diameter reinforcements.

Load (kN)	Disp (mm)		Load (kN)	Disp (mm)		Load (kN)	Disp (mm)	
	16 - 1	16 - 2		16 - 1	16 - 2		16 - 1	16 - 2
4.10	0.005	0.002	45.10	0.100	0.097	86.10	0.263	0.230
8.20	0.010	0.004	49.20	0.110	0.110	90.20	0.325	0.250
12.30	0.014	0.006	53.30	0.119	0.125	94.30	0.554	0.277
16.40	0.020	0.010	57.40	0.130	0.140	98.40	0.925	0.330
20.50	0.031	0.021	61.50	0.147	0.153	102.50	1.356	0.988
24.60	0.045	0.035	65.60	0.165	0.165	106.60	1.870	1.975
28.70	0.058	0.048	69.70	0.180	0.178	110.70	2.452	2.618
32.80	0.070	0.060	73.80	0.195	0.190	114.80	3.095	3.295
36.90	0.080	0.073	77.90	0.210	0.202	118.90	3.776	4.217
41.00	0.090	0.085	82.00	0.230	0.215	123.00	4.505	5.340

Table 4.2 : Observed displacements for the 20 mm diameter reinforcements.

Load (kN)	Disp (mm)		Load (kN)	Disp (mm)		Load (kN)	Disp (mm)	
	20 - 1	20 - 2		20 - 1	20 - 2		20 - 1	20 - 2
4.10	0.082	0.001	65.60	0.420	0.195	127.10	0.958	0.423
8.20	0.145	0.005	69.70	0.440	0.210	131.20	1.030	0.440
12.30	0.192	0.016	73.80	0.460	0.225	135.30	1.090	0.464
16.40	0.225	0.030	77.90	0.479	0.240	139.40	1.155	0.495
20.50	0.241	0.040	82.00	0.500	0.255	143.50	1.227	0.529
24.60	0.255	0.050	86.10	0.525	0.270	147.60	1.340	0.590
28.70	0.273	0.067	90.20	0.555	0.285	151.70	1.746	1.359
32.80	0.290	0.085	94.30	0.591	0.303	155.80	2.310	2.535
36.90	0.305	0.098	98.40	0.630	0.320	159.90	2.763	3.389
41.00	0.320	0.110	102.50	0.667	0.332	164.00	3.225	4.230
45.10	0.338	0.122	106.60	0.705	0.345	168.10	3.736	5.137
49.20	0.355	0.135	110.70	0.746	0.368	172.20	4.280	6.060
53.30	0.370	0.150	114.80	0.790	0.390	176.30	4.852	6.973
57.40	0.385	0.165	118.90	0.837	0.400	180.40	5.455	7.885
61.50	0.402	0.180	123.00	0.890	0.410			

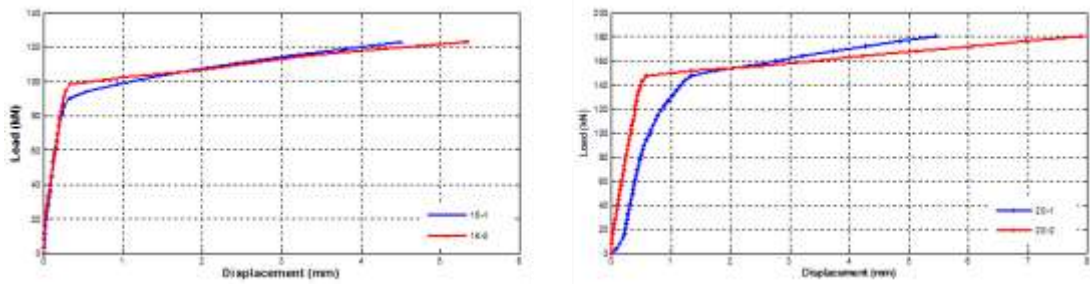


Figure 4.4 : Displacement-Load Curves.

As given in “Guideline for European Technical Approval of Metal Anchors for Use in Concrete Part Five: Bonded Anchors”; with bonded anchorages uncontrolled slip occurs when the mortar with the embedded part is pulled out of the drilled hole (because then the load displacement behavior depends significantly on irregularities of the drilled hole). The corresponding load when uncontrolled slip starts is called load at loss of adhesion N_{u_adh} . N_{u_adh} shall be evaluated for every test from the measured load displacement curve (EOTA, 2008) (Figure 4.5).

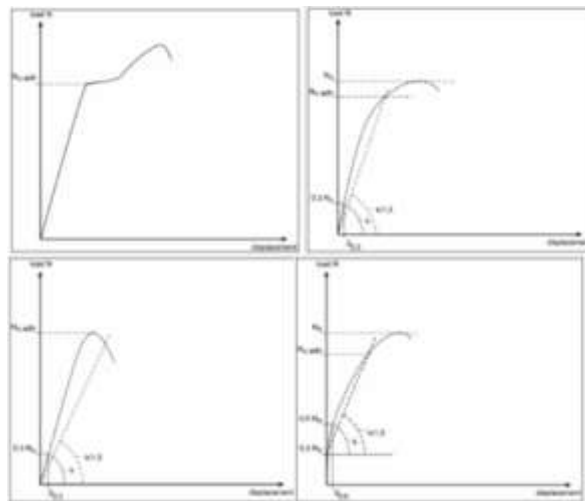


Figure 4.5 : Examples of load - displacements curves (EOTA, 2008).

By investigating the obtained load - displacement graphs of the reinforcements; it was observed that the acquired curves were seen to be similar with the first example given in ETAG Guideline, which means load at loss of adhesion by a significant change of stiffness. Although the reinforcements carries more load until pulling-out; the critical N_{u_adh} values and corresponding displacements were calculated and given in the below table (Table 4.3).

Table 4.3 : N_{u_adh} values and displacements.

Reinforcement	N_{u_adh} (kN)	Displacement (mm)
16 - 1	86.96	0.273
16 - 2	95.78	0.29
20 - 1	145.1	1.262
20 - 1	146.9	0.573

4.2 Network Design and Simulation for the Bridge

Istanbul has two suspension bridges which link the European and Asian parts of Istanbul and of Turkey. The second one, the Fatih Sultan Mehmet Bridge, is a modern type of suspension bridge. It is the 19th longest suspension bridge of the world. It started the public use in 1988. An immense level of transportation load comes to this bridge, since it lies on the “arteries” of the Turkish transportation net. The daily traffic of the bridge is approximately 180.000 vehicles. It spans 1510 meters from bank to bank. The distance between the two pairs of suspension towers is 1090 meters and towers are 105 meters above the roadway. The distance from the roadway carrier (lower edge) to the sea level is 64 meters (Apaydın and Erdik, 2001; Apaydın 2002).

After the earthquake occurred on 17th of August 1999, condition of the bridges became an important issue due to their major importance for the transportation. In connection, a seismic analysis project was implemented by the General Directorate of Highways. As a part of this project; a GPS monitoring campaign was held in July 2001. GPS observations with 0.1 seconds epoch interval were recorded for the same days of consecutive weeks. In addition, ancillary data such as traffic volume and weather conditions of the corresponding observation period were collected. The time series of the respective point displacements (deformations) were linked to the ancillary data. Then, in-depth analysis and comparison of the individual observation days was carried out. As the result of the study, a maximum of 40 mm height displacement within 13 seconds of periods was observed (Akyılmaz et al., 2004).

For the onsite monitoring of the bridge, an area just in front of the suspension towers of the European side was identified for the equipment installation. A reconnaissance fieldwork was performed to determine the feasible monitoring stations and targets. An initial map of the area was generated using the total station measurements (Figure 4.6). This information served as input to a photogrammetric network simulation

work. The proper camera locations, formats and lenses were interactively examined in the simulated environments. Three-camera based convergent multi-image acquisition geometry was adopted to provide adequate photogrammetric coverage of the experiment area.

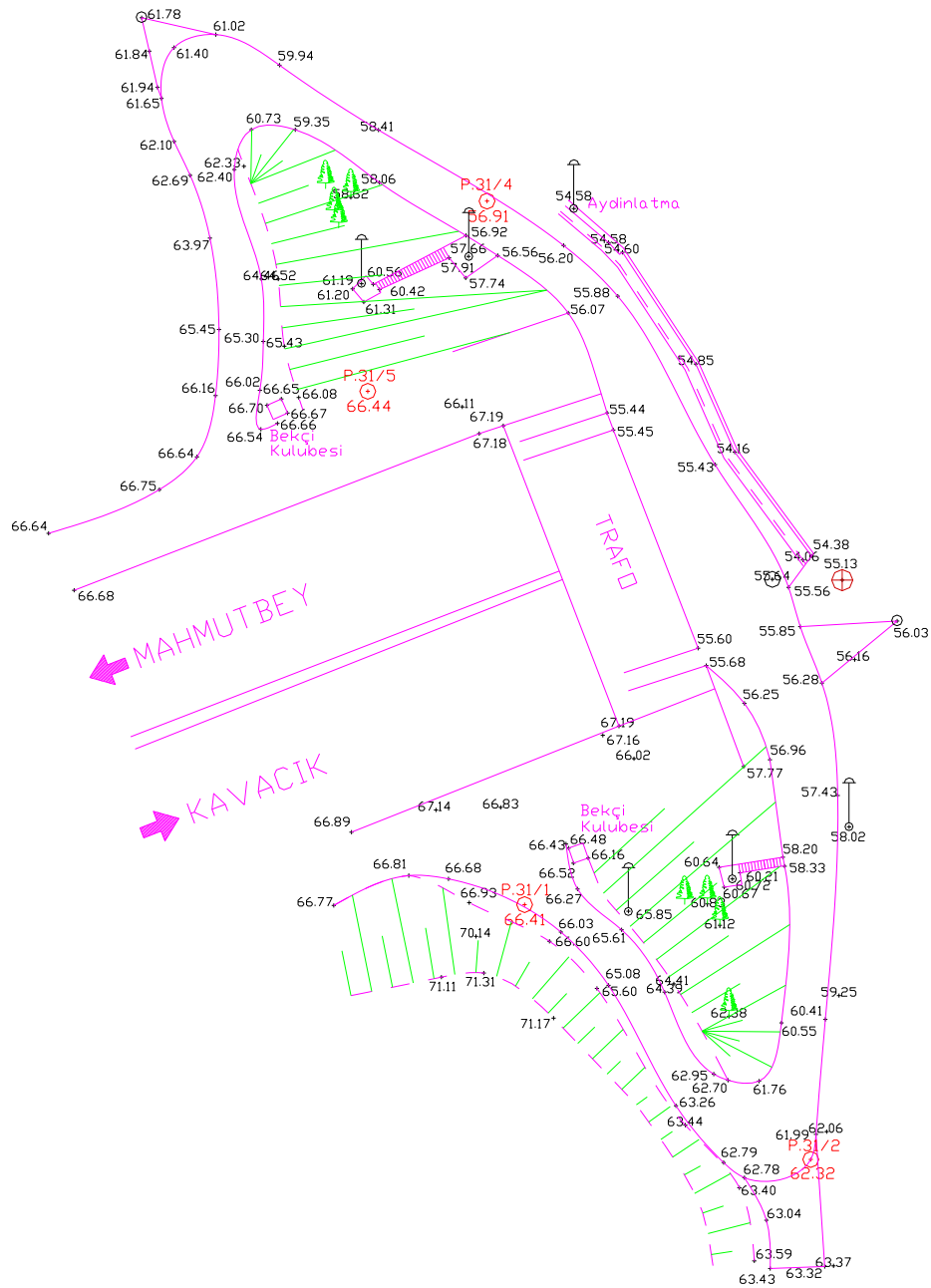


Figure 4.6 : Initial map of the area.

With the permission of GDH four pillars (Figure 4.7) were constructed on the application field. One of the pillars was set to be used for geodetic measurements and the rest were photogrammetric monitoring. Special apparatus for mounting camera holders to the pillar crests were manufactured and used.



Figure 4.7 : Pillars.

A system includes target, 12 volt accumulator for the energy, cable for flowing energy from the accumulator to the target and cable for charging the accumulator were designed and secured in a plastic box for portability. A total of 14 target points were affixed with using a chemical material to the lower surface of the bridge by using maintenance support platform (Figure 4.8).



Figure 4.8 : Targets.

A 2-day work was planned in the field and computers, cameras, power supplies and other equipment were located in the field. Since there is not long enough data cable; monitoring system was designed as 2 cameras were set to be controlled by one computer, the other camera was set to be controlled by a separate computer. Although the maximum resolution 2352 pixel x 1752 pixel, by considering the data storage capacity and time; a field of view with 2352*800 pixels were determined for region of interest since the other parts were not related to study area. 12 frames per second were set for image capturing and thus 2 seconds for image capturing and

approximately 5.5 seconds for data storing time was occurred. A data set includes the image and image taken time by the means of minutes, seconds and milliseconds. For image synchronization, a “for” loop was created that provides starting image acquisition at the same time for each cameras. This loop also provides advantage of parallel computing. By using the designed system 4800 data sets for the first day and 31968 data sets for the second day were obtained.

Subsequently data processing and evaluation step was began. For this purpose, In order to determine simultaneous images, an in-house developed algorithm that reads and matches the time component of the data was used. Image matching algorithms, explained in Section 3.3, were used to determine the targets on the images. Since searching a target in entire image will take too much time, image segmentation were applied to identify search areas. Since not the entire acquired image is necessary for the target recognition, a 121 pixel x 121 pixel areas were determined around the target points. Subsequently sub-pixel matching algorithms were used to determine the exact locations of the targets. By using the obtained pixel coordinates, image coordinates were calculated according to camera parameters acquired from the calibration.

To calculate the object coordinates of target points mathematical model of the photogrammetry that explains the relationship of the image and object coordinates, was used. However, since these formulas are not linear differential linear equations were used. Exterior orientation elements calculated in the previous steps were corrected iteratively and approximate target coordinates were measured by total station. Then graphs showing the displacements of each of the target points in all directions (x, y, z) are plotted.

4.3 Displacement Analysis of Suspension Bridges by Photogrammetry

The first day and the second day data sets were fully automatically measured in off-line mode. The average theoretical precision of the signaled points were computed as ± 72.4 mm, ± 19.9 mm, and ± 13.4 mm for the X, Y, and Z axes, respectively. The horizontal displacements of the two representative targets are given in following figure (Figure 4.9, Figure 4.10).

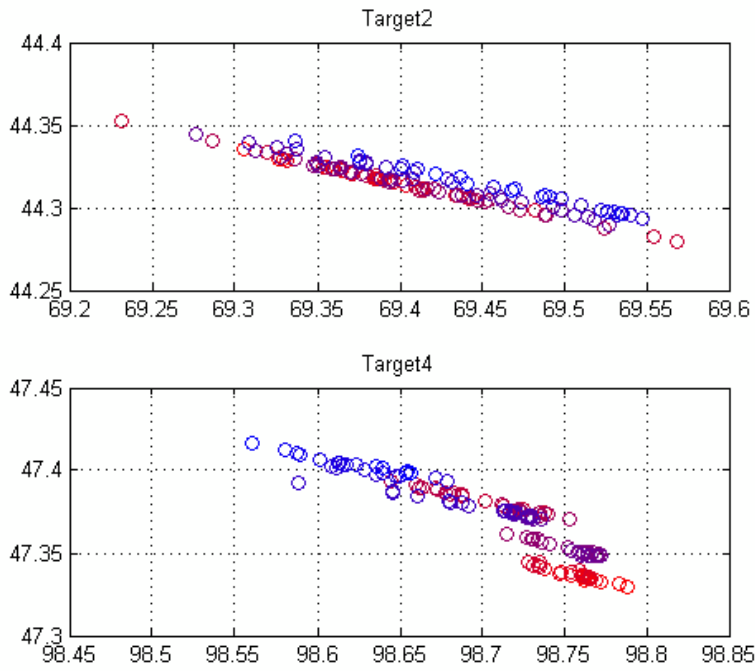


Figure 4.9 : The horizontal displacement of Target 2 and 4.

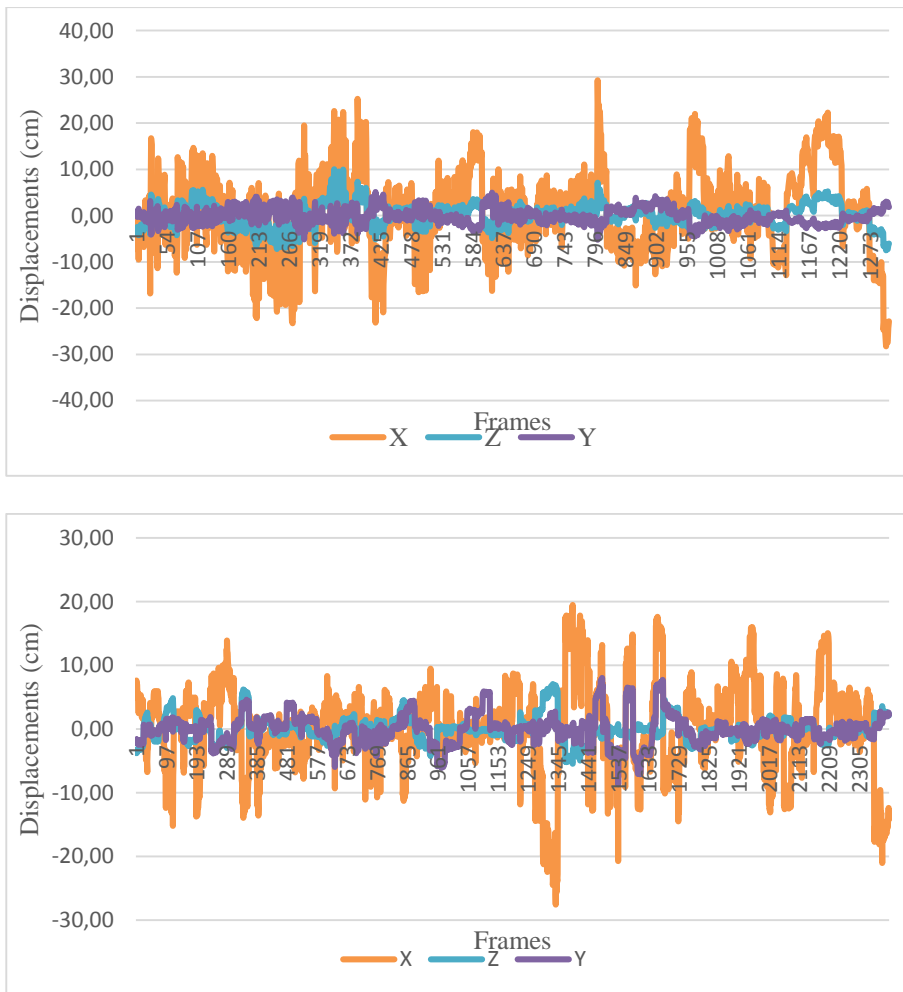


Figure 4.10 : The total displacement of Target 2 and 4.

5. CONCLUSIONS

Bridges are exposed to intensive and dynamic loads, unsteady weather conditions, material fatigue and aging process. All these factors cause deformations on the construction parts. The importance of the monitoring and early identifying the bridge deformations is essential once the maintenance, repair and even the reconstruction costs are considered. Monitoring campaigns of long bridges are becoming more and more common as the research fields of structural health monitoring and performance monitoring grow. This thesis aimed to propose a photogrammetric monitoring network that includes the steps from acquisition to analysis.

Therefore, the very first step was the determination of camera lens set that would provide the necessary field of view and accuracy. Furthermore, a Matlab based software suit was specifically developed for image acquisition and synchronization.

The indoor tests were applied to discover and improve the deficiencies of the system. Since the main movement of the bridge is oscillation, a pendulum was settled up and monitored at the photogrammetry laboratory of the Geomatics Engineering Department.

For understanding the availability of monitoring displacements of an object, the second indoor test, which installed in the Construction Materials Laboratory of Istanbul Technical University, implemented pull-out deformations test of bonded metal anchors embedded in concrete.

On the other hand, a Matlab based photogrammetric evaluation suit was developed to process orientation, matching, positioning and visualization and performed on the indoor tests.

Hence the accomplished results of the indoor tests, it was decided to investigate the system on fieldwork. Due to its importance, Second Bosphorus Bridge was selected as the main object. In this study, three still video cameras were used to monitor the movement of the bridge platform. From three imaging stations the first 150 meters of

the bridge body was monitored using the photogrammetric technique with a 2352 x 800 pixels field of view and 12 fps image acquisition frequency.

In the future work, further analysis steps will be performed by inspecting transportation load and weather (wind and temperature) conditions. This research can be extended to monitor the entire bridge with an on-line photogrammetric monitoring and evaluation system.

REFERENCES

- ACI Committee 355** (1991). State-of-The-Art-Report on Anchorage to Concrete, ACI 355.1R-91, *American Concrete Institute*, Detroit.
- Albert, J., Maas, H.-G., Schade, A., Schwarz, W.** (2002). Pilot studies on photogrammetric bridge deformation measurement, *Proceedings of the 2nd IAG Commission IV Symposium on Geodesy for Geotechnical and Structural Engineering*, 21–24 May, Berlin, Germany.
- Akyilmaz O., Çelik R. N., Apaydın N., Ayan T.** (2004). GPS Monitoring of the Fatih Sultan Mehmet Suspension Bridge by Using Assessment Methods of Neural Networks, *The International Archives of the Photogrammetry, Remote Sensing and Spatial Information Sciences*, Istanbul, Turkey XXXV. Part B7, 702-707.
- Amiri Parian, J., Gruen, A. and Cozzani, A.** (2007). Monitoring of the reflectors of ESA's Planck telescope by close-range photogrammetry. *Journal of Applied Geodesy*, 1(3): 137–145.
- Apaydın N.** (2002). Seismic Analysis of Fatih Sultan Mehmet Suspension Bridge, *Ph.D. Thesis*, Department of Civil Engineering, Boğaziçi University, Istanbul, Turkey.
- Apaydın N., Erdik M.** (2001). Structural Vibration Monitoring System for the Bosphorus Suspension Bridges, *Strong Motion Instrumentation for Civil Engineering Structures*, Kluwer Academic Publishers, pp. 343-367.
- Bales, F.B., Hilton, M.H.** (1985). Application of Close-range Terrestrial Photogrammetry to Bridge Structures, *Virginia Highway and Transportation Research Council*.
- Barazzetti, L., Scaioni, M.** (2010). Development and Implementation of Image-based Algorithms for Measurement of Deformations in Material Testing, *Sensors 2010*, 10, 7469-7495; doi: 10.3390/s100807469.
- Bogatin S., Foppe K., Wasmeier P., Wunderlich T. A., Schafer T., Kogoj D.** (2008). "Evaluation of linear Kalman filter processing geodetic kinematic measurements" *Measurement*, 41: 561–578.
- D'Apuzzo, N.** (2003). "Surface measurement and tracking of human body parts from multi station video sequences", *Ph.D. Thesis*, Nr. 15271, Institute of Geodesy and Photogrammetry, ETH Zurich, Switzerland.
- Debella-Gilo, M., Käab A.** (2011). Sub-pixel precision image matching for measuring surface displacements on mass movements using normalized cross-correlation, *Remote Sensing of Environment*, Volume 115, Issue 1, 17 January, 130–142.

- European Organisation for Technical Approvals** (2008). ETAG 001, Edition March 2002, *Guideline For European Technical Approval Of Metal Anchors For Use In Concrete*, Amended November 2006, Second Amendment February 2008, Part Five: Bonded Anchors.
- Fraser, C. S.** (1997). Digital Camera Self Calibration, *ISPRS Journal of Photogrammetry and Remote Sensing*, 52, No. 4, pp.149-159.
- Fraser, C.S., Riedel, B.** (2000). Monitoring the thermal deformation of steel beams via vision metrology, *ISPRS Journal of Photogrammetry & Remote Sensing*, 55 (4) 268–276.
- Gowwald, R.** (1987) Kern E2-SE – Ein neues Instrument nicht nur für die Industrievermessung?, *Allgemeine Vermessungs-Nachrichten (AVN)*, No. 4, 147.
- Habib, A. and Morgan, M.** (2003). Automatic calibration of low-cost digital cameras, *Journal of Optical Engineering*, 42(4), 948-955.
- Hegger, J., Sherif, A., Gortz, S.** (2004). Investigation of pre- and post-cracking shear behavior of prestressed concrete beams using innovative measuring techniques, *ACI Structural Journal*, 101 (2) 183–192.
- Johnson, G.W.** (2001). Digital close range photogrammetry – a portable measurement tool for public works. *Coordinate Measurement Systems Committee Conference*, Albuquerque, NM, 13–17 August.
- Ja'uregui, D.V., White, K.R., Woodward, C.B., Leitch, K.R.** (2003). Noncontact photogrammetric measurement of vertical bridge deflection, *Journal of Bridge Engineering*, 8 (4) 212–222.
- Kalkan, Y., Alkan, R.M. and Bilgi, S.** (2010). "Deformation Monitoring Studies at Atatürk Dam", Proc. on XXIV. *FIG International Congress 2010*, Sydney, Australia, 11-16 April.
- Katowski, O.** (1989) Deformationsmessung an Bauwerken mit dem automatischen Theodolitmess-System ATMS, *Proceedings of Optical 3-D Measurement Techniques*, 393-403.
- Kaya, Y.** (2007). Pull-out behavior of partially bonded anchors to be used in retrofitting existing structures under anchorage interface conditions, MsC Thesis, ITU Institute for Science and Technology, 2007, Istanbul, Turkey.
- Kim, B.G.** (1989). Development of a photogrammetric system for monitoring structural deformations of the sturgeon bay bridge, *PhD Dissertation*, University of Wisconsin, Madison.
- Koo KY, Brownjohn JMW, List D, Cole R, Wood T.** (2010). Innovative structural health monitoring for Tamar Suspension Bridge by automated Total Positioning System, Bridge Maintenance, Safety, Management and Life-Cycle Optimization - *Proceedings of the 5th International Conference on Bridge Maintenance, Safety and Management*, 556-563.
- Koo K. Y., Brownjohn J. M. W., List D. I., Cole R.** (2013). Structural health monitoring of the Tamar suspension bridge, *Structural Control and Health Monitoring*, volume 20, no. 4, 609-625.

- Leitch, K.R.** (2002). Close-range photogrammetric measurement of bridge deformations. *Ph.D. Dissertation*, Civil and Geological Engineering Department, New Mexico State University, Las Cruces, New Mexico.
- Maas, H.-G.** (2006). Photogrammetric Techniques in Civil Engineering Material Testing and Structure Monitoring, *Photogrammetric Engineering & Remote Sensing* Vol. 72, No. 1, January 2006, 39–45.
- Maas, H.-G., and Niederöst M.** (1997). The accuracy potential of large format still video cameras, *Videometrics V* (S. El Hakim, editor), SPIE Proceedings Series, Volume 3174.
- Reiterer, A., Huber, N. B., Bauer, A.** (2010). Image-Based Point Detection and Matching in a Geo-Monitoring System, *Allgemeine Vermessungsnachrichten (AVN)*, No. 4, 129-139.
- Remondino, F.** (2004). 3-D Reconstruction of static human body shape from image sequence. *Computer Vision and Image Understanding*, Vol. 93(1), 65-85
- Scherer, M.** (2004). Intelligent Scanning with Robot-Tacheometer and Image Processing a Low Cost Alternative to 3D Laser Scanning, *Proceedings of the FIG Working Week*, Athens, Greece.
- Wagner, A., Wasmeier, P., Reith, C., Wunderlich, T.** (2013). Bridge Monitoring By Means Of Video-Tacheometer – A Case Study, *Allgemeine Vermessungs-Nachrichten (AVN)*, 283-292.
- Walser, B. H.** (2004). Development and Calibration of an Image Assisted Total Station. *PhD Thesis*, ETH-Zürich.
- Wasmeier, P.** (2009). Grundlagen der Deformationsbestimmung mit Messdaten bildgebender Tachymeter. *PhD Thesis*, Technische Universität München.
- Yilmaz, S., Caliskan, O., Kaplan, H., Kirac, N.** (2010). Factors Affecting the Strength of Chemical Anchors, *Journal of Engineering and Architecture Faculty of Eskisehir Osmangazi University*, Vol: XXIII, No:1.
- Yong-Qi, C.** (1983). Analysis of Deformation Surveys - A Generalized Method, Technical Report No. 94, University Of New Brunswick, Latest Reprinting September 1996
- Zogg, H.-M., Ingensand H.** (2008). Terrestrial Laser Scanning For Deformation Monitoring - Load Tests on The Felsenau Viaduct (CH), *The International Archives of the Photogrammetry, Remote Sensing and Spatial Information Sciences*, Beijing, China Vol. XXXVII. Part B5, 555-561.

CURRICULUM VITAE



Name Surname: Emin Özgür AVŞAR

Place and Date of Birth: Samsun, 1980

Address: Istanbul Technical University, Faculty of Civil Engineering, Department of Geomatics Engineering, 34469, Maslak, İstanbul / Turkey

E-Mail: avsarem@itu.edu.tr

B.Sc.: Geodesy and Photogrammetry Engineering at ITU Civil Engineering Faculty

M.Sc.: Geomatics Engineering at ITU Institute of Science and Technology

Professional Experience and Rewards:

Worked as a Research Assistant at ITU Department of Geomatics between 2005-2012

List of Publications and Patents:

International Conference Papers

- Kaya, S., Bozkurtoglu E., **Avsar E. Ö.**, Aydar U., Seker, D. Z. (2011). Determination of Roughness Angles of Surfaces Using Laser Scanner, *FIG Working Week – Bridging the Gap Between Cultures*, 18–22 May 2011, Marrakech, Morocco
- **Avşar E. Ö.**, Duran Z., Akyol O., Toz G. (2008). Modeling of the Temple of Apollo Smintheus Using Photogrammetry, Laser Scanning and Virtual Realty, *XXI. ISPRS Congress*, 03–11 July 2008, Beijing, China
- Aydar, U., **Avşar, E. Ö.**, Altan, M. O. (2007). Obtaining Façade Plan of a Historical Building with Orthorectification of Single Images Gathered by Mobile Phones, Digital- and Video-Cameras, *XXI CIPA International Symposium*, 1–6 Kasım 2007, Atina, Yunanistan
- Seker, D.Z., **Avşar, E. Ö.**, Aydar, U. (2006). Modeling of Historical Bridges Using Photogrammetry and Virtual Realty, *FIG XXIII Congress and XXIX General Assembly - Shaping the Change*, 8–13 Ekim 2006, Münih, Almanya

- **Avşar, E. Ö.**, Aydar, U., Seker, D.Z. (2006). Virtual Reconstruction of a Semi Destroyed Historical Bridge, *5th Turkish-German Joint Geodetic Days*, 29–31 Mart 2006, Berlin, Almanya
- **Avşar, E. Ö.**, Duran, Z., Seker, D. Z., Hisir, M., Shrestha, M. (2004). GIS Based Natural Disaster Mapping: A Case Study, *XX. ISPRS Congress*, 12–23 Temmuz 2004, İstanbul, Turkey.

National Conference Papers

- Çelik, M. F. Küçükosman, G., Yüksel, E., Duran, Z., Aydar, U., **Avşar, E. Ö.** (2013). Lazer Tarayıcı Yardımı ile Üç Boyutlu İç Mekan Modeli Oluşturulması ve Coğrafi Bilgi Sistemine Aktarılması, *TMMOB Coğrafi Bilgi Sistemleri Kongresi 2013*, 11-13 Kasım 2013, Ankara
- Akay S.S., Uzun G., Duran Z., **Avşar E. Ö.**, Aydar U. (2012). Lazer Tarama Yöntemi İle Elde Edilen Üç Boyutlu Mekân Modellerinin Coğrafi Bilgi Sistemlerinde Kullanım Olanakları, *IV. Uzaktan Algılama ve Coğrafi Bilgi Sistemleri Sempozyumu*, 16-19 Ekim 2012, Zonguldak
- Uzun, G., Akay, S. S., Duran, Z., Aydar, U., **Avşar, E. Ö.** (2012) Üç Boyutlu İç Mekân Modelinin Yersel Lazer Tarama Yöntemi İle Elde Edilmesi Örneği, *6. Mühendislik Ölçmeleri Sempozyumu*, 3-5 Ekim 2012, Afyon
- **Avşar, E. Ö.**, Aydar, U., Şeker, D. Z. (2011). İTÜ Geomatik Mühendisliği Bölümünde Kültürel Mirasın Dokümantasyonuna Yönelik Olarak Öğretilen Yöntemler ve Yersel Fotogrametri Eğitimi, *TMMOB Harita ve Kadastro Mühendisleri Odası, 13. Türkiye Harita Bilimsel ve Teknik Kurultayı*, 18–22 Nisan 2011, Ankara
- Kaya, Ş., Bozkurtoğlu, E., **Avşar, E. Ö.**, Aydar, U., Şeker, D. Z. (2011). Yüzeylerin Pürüzlülük Açısının Lazer Tarayıcılar Yardımıyla Belirlenmesi, *TMMOB Harita ve Kadastro Mühendisleri Odası, 13. Türkiye Harita Bilimsel ve Teknik Kurultayı*, 18–22 Nisan 2011, Ankara
- **Avşar, E. Ö.**, Aydar, U., Duran, Z., Arpacı, K. E., Digital Fotogrametri Tekniği Yardımıyla İç Mekan Modellemesi ve Web Tabanlı Sunulması, *TMMOB Harita ve Kadastro Mühendisleri Odası, 12. Türkiye Harita Bilimsel ve Teknik Kurultayı*, 11–15 Mayıs 2009, Ankara
- Altan, O., Külür, S., Toz, G., Şeker, D. Z., Demirel, H., Duran, Z., Akçay, Ö., **Avşar, E. Ö.**, Aydar, U. (2008). Tarihi Kent Dokusunun Korunmasında Fotogrametrinin Kullanım Olanakları, *Kent Yönetimi, İnsan ve Çevre Sorunları '08 Sempozyumu*, 02-06 Kasım 2008, İstanbul
- Vatansever, C., Yardımcı, N., **Avşar, E. Ö.**, Aydar, U., Şeker, D. Z. (2007). İnce Çelik Levhalı Perdede Levhanın Düzlemdışı Hareketlerinin Fotogrametri İle Belirlenmesi, *Türkiye Ulusal Fotogrametri ve Uzaktan Algılama Birliği IV. Teknik Sempozyumu*, 5–7 Haziran 2007, İstanbul

- **Avşar, E. Ö.**, Aydar, U., Şeker, D. Z. (2007). Tarihi Köprülerin Digital Fotogrametri Tekniği Yardımıyla Modellenmesi, *TMMOB Harita ve Kadastro Mühendisleri Odası, 11. Türkiye Harita Bilimsel ve Teknik Kurultayı, 2-6 Nisan 2007*, Ankara
- Girişken, M. U., Akkoca, G., **Avşar, E. Ö.**, Ayhan, E., Şatıroğlu, A., Doğru, A. Ö. (2007). Jeodezi ve Fotogrametri Mühendisliği Öğrencilerinin Dünyadaki Örgütlenmesi, *TMMOB Harita ve Kadastro Mühendisleri Odası, 10. Türkiye Harita Bilimsel ve Teknik Kurultayı, 2-6 Nisan 2007*, Ankara

PUBLICATIONS/PRESENTATIONS ON THE THESIS

- **Avşar, E. Ö.**, Akca, D., Altan, O. (2014). Determining Pull-Out Deformations by means of an Online Photogrammetry Monitoring System, *International Journal of Environment and Geoinformatics*, Vol 2, 2014
- **Avşar, E. Ö.**, Akca, D., Altan, O. (2014). Photogrammetric Deformation Monitoring of the Second Bosphorus Bridge in Istanbul, *ISPRS Technical Commission V Symposium, 23-25 Jun 2014*, Riva, Italy
- **Avşar, E. Ö.**, Dogan, U. A., Altan, O. Akca, D. (2012). Determining Pull-out Deformations of Bonded Metal Anchors Embedded in Concrete by Means of Photogrammetry, *XXII. ISPRS Congress, 25 August-01 September 2012*, Melbourne, Australia
- Aydar, U., **Avşar, E. Ö.**, Kaya, Ş., Bozkurtoğlu, E., Şeker, D.Z. (2011). Yüzeylerin Pürüzlülük Açılarının Lazer Tarayıcılar Yardımıyla Belirlenmesi, *hkm Jeodezi, Jeoinformasyon ve Arazi Yönetimi Dergisi 2011/2 Özel Sayı*, Sayı: 105, sh. 33-38.

